

Size-exclusion chromatography on soft packing material under axial compression

A.V. Danilov, L.G. Mustaeva, I.V. Vagenina, M.B. Baru*

Branch of Shemyakin and Ovchinnikov Institute of Bioorganic Chemistry, Russian Academy of Sciences, Puschino, 142292 Moscow Region, Russia

Received 4 October 1995; accepted 3 November 1995

Abstract

The influence of soft gel axial compression on the packing structure and the associated chromatographic parameters such as dispersion of chromatographic zones, retention volume and peak resolution have been considered for size-exclusion chromatography. Continuous time gel compression is accomplished by the use of a special column with controlled external pressure applied to the packing. The experimentally obtained improvement in resolution combined with the decrease in separation time has been proved.

Keywords: Axial compression; Stationary phases, LC; Band broadening

1. Introduction

Conventional LC remains a common method of isolation and purification of biological substances, even in a period of great progress in analytical and preparative HPLC and associated methods. Features peculiar to biological substances may favour LC as labile, water soluble biospecies require extreme care in handling.

It is worth mentioning that in the conventional LC of biomolecules most attention is given to the development of highly efficient packing materials which are derived mainly from polymeric gels or composite materials. Manufacturers have modified most of the parameters of solid phases which are directly related to packing selectivity: chemical structure of sorption sites, sorption capacity, the

accessibility of pores and the flexibility of a polymer (see the survey in Ref. [1] for details).

In parallel with selectivity effectiveness inherent to a packed bed (responsible for band broadening) influences resolution in LC. Therefore a user faces the problem of obtaining a high-quality packing in a column and ensuring its stability in the course of a separation process. Despite the great variety of columns for the LC of biopolymers that are commercially available, slurry packing in aqueous media by sedimentation and/or by flow still remains as the main method of packing. While high pressures several times greater than the operating pressures are applied during slurry packing of rigid particles (such as silica-based particles), in the case of xerogels (such as dextran- or polyacrylamid-based matrixes, etc.) maximum flow-rates (and the corresponding pressures) are close to the recommended operating flow-rates (which are rather low). This results in a

*Corresponding author.

long packing time, and undesirable redistribution of gel beads, according to size, along the column axis becomes more probable. On the other hand, packing pressure can be insufficient to achieve a completely homogeneous packed bed.

Much attention is paid to packing procedures and packed bed stability in preparative HPLC [2–4], the separation efficiency being one of the decisive factors in the price of a particular product. It has been shown that, beginning with a definite I.D., columns of the conventional type are less stable than analytical-sized columns. That I.D. value is dictated by the packing material as well as the mobile phase type, for instance a column with I.D. more than 22 mm appears to be unstable when packed with 10- μm reversed-phase silica gel [5]. It is believed [6] that a packed bed may contain loose, i.e. unstable, regions where microvoids are formed. Beads rearrange gradually with time and the whole bed settles giving channels or voids at the column inlet. This may be caused by repeated thermal expansion/contraction of the packing bed, pump pulsations, etc. The influence of I.D. value on these effects is caused by the decrease in column wall support.

Since the difference between HPLC and low pressure chromatography appears to be quantitative rather than qualitative, similar phenomena also take place with the use of soft packing materials. Only variations in their values and duration are observed. The capacity of xerogels for mechanical deformation (for instance under the action of liquid flow or owing to variations in swelling in the gradient elution mode) seems to increase the probability of such occurrences (compared to aerogels) and also to cause a decrease in the effect of the column walls which stabilizes a packing for analytical columns with rigid gel packings.

Packing improvement and stabilization can be attained by adapting the column volume to the changing bed volume. Axial and/or radial compression applied during a chromatographic process make such adaptation possible. HPLC instruments based on both approaches are now commercially available from a number of manufacturers [3]. The designs of choice are those utilizing the dynamic mode of compression [7,8]. Summing up the results of the studies on the performances of spherical and angular silica-based packings in dynamic compression col-

umns [6,9–11], the following advantages of the latter packings can be mentioned: (i) packing procedure convenience and the possibility to repack; (ii) prevention of void formation and long-term stability; (iii) high column efficiency with low mass transfer limitation. (The only disadvantage is their higher price).

Similar designs are also used in preparative low-pressure chromatography. For instance, axial packing technology with a 700-kPa pressure rating is used for VantageTM columns for biochromatography (Grace Industrial, Lausanne, Switzerland). This results in higher flow-rates, improved column bed stability and faster throughput. “Automatic Bed Height Column” (e.g. Model ABHC440x500) manufactured by Amicon (Danvers, MA, USA) is an example of the application of compression to packed beds that change their volume in the course of chromatographic procedures. This column is designed to provide a slight gas overpressure (0.5–5 p.s.i.) to the sealed space above the adjuster assembly. The resulting advantages may be summarized as follows: easier packing and regeneration, better resolution due to minimal dead volume.

However variations in chromatographic characteristics of soft gel packing resulting from its compression have not been adequately investigated (in contrast to rigid packings) although the “dead volume” minimization inevitably involves such variations. It should be noted that, in 1970, Edwards and Heft demonstrated the improved separation of Blue Dextran 2000 and $\text{Ni}(\text{NO}_3)_2$ on Sephadex G-50 under compression [12]. With their method of packing, compression by the action of the hydraulic pressure of the eluent involves an increase in the linear flow-rate of the eluent and this is accompanied by a reduction in the efficiency. Thus it is difficult to predict the packing behaviour under further compression because of the two counteracting processes.

We have already shown previously [13] that ion-exchange separation on “soft” CM Sephadex C-25 improves under axial compression. Compression has been achieved by the use of a special refinement in the design of a standard Pharmacia column. The gel packing remains under dynamic axial compression throughout the process.

A detailed examination of the parameters of soft packing materials under dynamic compression is the

objective of our study. Size-exclusion chromatography (SEC) has been chosen for the investigation as SEC packing geometrical parameters (which are for the most part influenced by compression) affect peak retention and dispersion.

2. Experimental

2.1. Apparatus and reagents

The chromatographic system consisted of a 2150 HPLC pump (LKB, Sweden), a sample injector V-7 (Pharmacia, Sweden) with 250- μ l loop, an original column of variable volume, an ultraviolet photometric detector 2238 Uvicord SII and a 2210 two-channel recorder (LKB, Sweden). All chemicals were of analytical grade. Sephadex G-25 SF and Blue Dextran 2000 were obtained from Pharmacia (Sweden).

2.2. Design of the column with axial compression

SEC separation of the Blue Dextran (BD) and potassium dichromate (PD) mixture was performed on a column of an original design similar to the one described in our previous publications [14,15]. The column was a precision-bore glass cylinder (10 mm I.D.) with the high inner surface finish. The inner surface was carefully silanized to diminish friction. The key unit of the column was a floating piston (FP). The design of a Teflon FP seal made it possible to minimize friction. To compress the packed bed continuously, the FP was subjected to the action of an external force in the axial direction. To do this we used a system of variable weights. For convenience, the weights–FP connection was made as a detachable joint.

2.3. Procedures

A commercial dextran gel (Sephadex G-25 SF grade) was used. The gel slurry, previously swollen in water, was poured into the column. When the packing height became constant the FP was inserted and further bed consolidation was accomplished by axial compression with an appropriate load, the

eluent being continuously supplied to the column at the operating flow-rate.

Operating compression of the gel packing was set up to 300 kPa. It is worth mentioning that there were no experiments with zero compression. It is impossible to determine the value and direction of friction between the FP and the column walls at rest (when compression is counteracted by the gel packing). That is why the experiments have been carried out starting from 38 kPa compression in order to reduce the uncertainty. Initially the compression increase causes local deformation of the gel particles near the FP due to an additional load. In order to provide uniform distribution of this deformation all over the gel bed, the column was washed overnight. After the packing had been consolidated, a sample of 250 μ l of distilled water containing 0.2% (w/v) BD and 0.1% (w/v) PD was applied to the column with an injection valve. Distilled water elution was performed at a flow-rate of 0.3 ml/min at ambient temperature. The substances were spectrophotometrically detected at 226 nm.

The column design enabled visual inspection of variations in the bed height and their measurement in the course of contraction.

2.4. Data acquisition

Experimental data acquisition was made with DOS-based software written in BASIC in our laboratory.

The retention volume of the peaks was calculated as the first moment, μ_1 . Band broadening was expressed according to the standard method of calculation of the peak second central moment, μ_2 . In the calculations, both moments have been corrected for the finite volume of the injected sample. The dispersion of the leading (σ^2) and rear (τ^2) peak edges relative to the elution volumes of peak maxima, V_M , has been calculated according to Eq. 1 and Eq. 2, respectively:

$$\sigma^2 = \sum_j h_j (V_j - V_M)^2 / \sum_j h_j, \text{ at } V_j < V_M \quad (1)$$

$$\tau^2 = \sum_j h_j (V_j - V_M)^2 / \sum_j h_j, \text{ at } V_j > V_M \quad (2)$$

where h_j and V_j are the detector response and the

volume corresponding to effluent fraction j , respectively.

The error values estimated as the least squares deviation from regression analysis did not exceed 6% and 6% for μ_1 and μ_2 respectively in case of BD and 9% and 5% for the described moments in the case of PD.

3. Results and discussion

3.1. Mechanical properties and internal geometry of the packing

The externally applied compressive force causes internal reactive forces in a deformed gel bed and the associated volume changes. The elastic behaviour of the packed bed must depend on the mechanical properties of gel beads as well as on their arrangement in space and friction on each other. Fig. 1 shows the experimental relationship between the gel bed height L and the pressure applied. Though a packed bed is not a solid, its mechanical properties appear to be similar to those of elastic solids judging by the curve, so

$$F/S = P \approx -E \Delta L/L_0, \quad (3)$$

where S is the column cross-section area, F and P

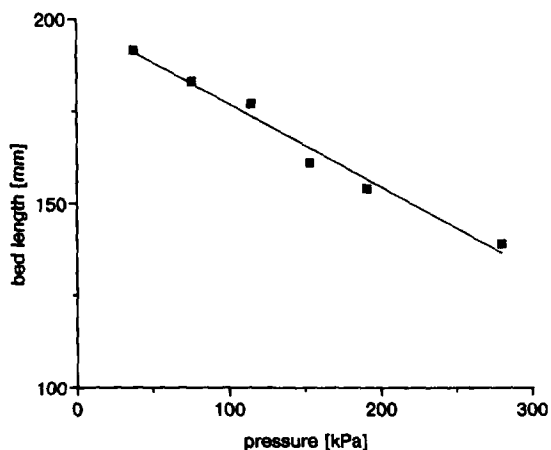


Fig. 1. Bed height versus axial compression: the line corresponds to linear regression fit.

are the force and pressure of compression, respectively, and $\Delta L/L_0$ is the relative deformation of the gel packing. Calculated by Eq. 3, the modulus of elasticity, E , is approximately equal to $9 \cdot 10^5 \text{ N m}^{-2}$ (for comparison the corresponding value for rubber is an order of magnitude higher).

It is worth mentioning that the gel bed experiences deformation gradually. It has taken a long time (about several hours) for the gel bed to stabilize after the compression increase in the course of the described experiment. Similar phenomena take place in rigid packing materials [8]. Thus damped stabilization of an angular 10- μm silica packed bed was observed over 100 h. The rearrangement of the bed under compression due to the collapse of the unstable regions created during the packing step provides an explanation for such damped stabilization. Deformation of rigid silica-based packings upon axial compression seems to be irreversible; indirect evidence can be found in the data of Wu and Lohse [10]. They ran an experiment to elucidate the influence of successively decreased compression on the column performance of silica packing. No effect on the column efficiency and back-pressure was observed with a four-fold decrease in compression from its maximum value, indicating that the bed was very stable.

In contrast, an increase in the bed height was observed upon instantaneous Sephadex packing decompression (from 280 kPa to zero), though the process was slow. The residual deformation after complete relaxation was approximately 50% of the initial value (that of deformation at 280 kPa). Therefore partial reversibility of the compression effect on soft packing materials such as dextran-based ones has been observed. Microscopic studies of sampled gel beads did not reveal any substantial changes in their spherical form and the quantity of destroyed beads did not exceed 1–2% of their total quantity.

In view of BD total exclusion from the gel particles of Sephadex G-25, its retention volume (μ_1^0) must correspond to the moving mobile phase column volume, V_0 . The retention volume of totally penetrating PD (μ_1^1) is equal to the total liquid phase column volume, V_t , accordingly. Thus the inner volume of gel packing V_i is equal to $\mu_1^1 - \mu_1^0$. Typical curves corresponding to V_0 , V_t and V_i under packing

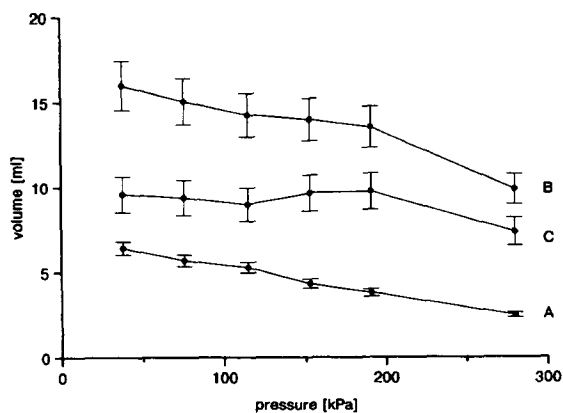


Fig. 2. Effect of axial compression on SEC retention volumes (A) V_0 , (B) V_R , (C) $V_i = V_i - V_0$.

compression are shown in Fig. 2. While the decrease in V_0 is almost linear with the rise in P , the decrease in V_i starts at more than 200 kPa compression. It is represented by the sigmoid shape of the V_i/V_0 curve (Fig. 3), V_i/V_0 being the ratio of pore volume to void volume.

The second curve in Fig. 3 also illustrates the variation of another dimensionless parameter V_0/V_t , that is almost equal to the inter-particle porosity of gel packing. The V_0/V_t value varies from 0.40 to 0.25 with the increase in compression from 38 to 280 kPa. The resulting porosity value corresponds to the value

for maximum packing density of incompressible spheres of equal size (rhombohedral and face-centered cubic array).

Sephadex compression may be supposed to result not only in the rearrangement of the packed bed into a tighter array but also in the deformation of the particles themselves. The latter phenomenon is supported by the decrease in the V_i value (at pressures above 200 kPa) and reversibility of bed deformation. Slow and incomplete restoration of the bed height can be attributed to the generation of a new packing structure more compact than the initial one and also to a residual deformation of beads that persists under the action of inter-particle friction. Unfortunately, the precise determination of the prevailing process upon a compression of particular value is not possible with the data obtained.

3.2. Band broadening upon packing compression

The elution profiles in Fig. 4 corresponding to the initial and maximum values of Sephadex packing compression indicate a decrease in retention volumes in parallel with the reduction in the width of peaks. The influence of the packing compression on band broadening is depicted in Fig. 5.

Analysis of the data presented in Fig. 2 and Fig. 5 suggests different results for compression in the case

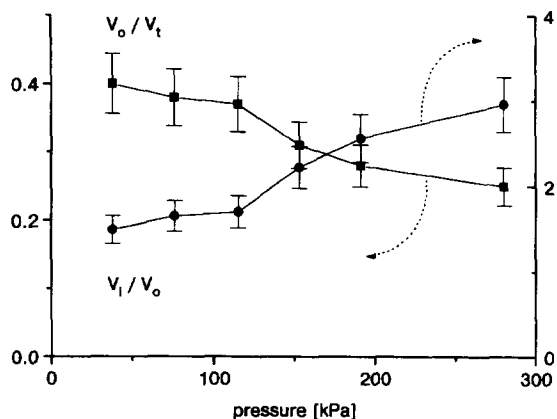


Fig. 3. Effect of axial compression on packing parameters V_i/V_0 and V_0/V_t .

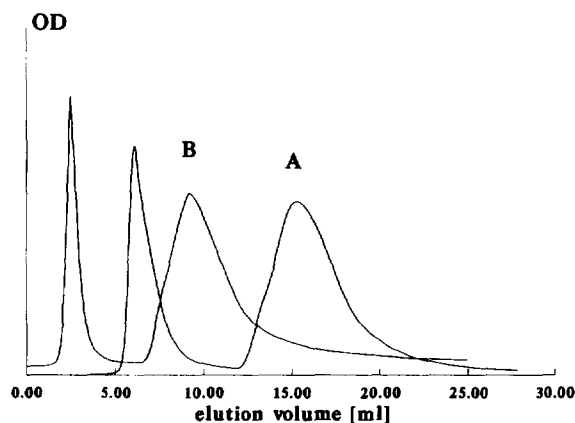


Fig. 4. Elution profiles obtained upon 38 kPa (A) and 280 kPa (B) compression pressure.

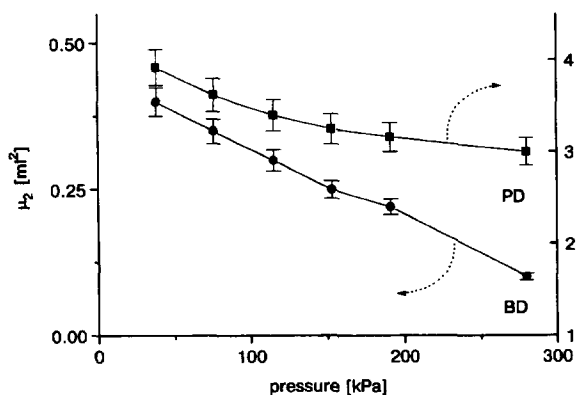


Fig. 5. Peak variance versus axial compression.

under consideration (SEC on soft packing) and in chromatographic separations on silica-based packings. As SEC separation is caused by the distinction in distribution of substances between mobile and stagnant liquid phases, volume variations of the latter upon compression influence the efficiency of the method significantly. That was the case in our experiment, as μ_1 and μ_2 variations were comparable to their initial values in order of magnitude (61% and 75% of their initial values for BD and 38% and 23% for PD respectively). The retention variation as such upon axial or radial compression of rigid silica-based particles is not reported in the literature. Thus the negligibility of this effect can be indirectly deduced for the latter case (see Ref. [10] for example).

As already discussed (see Fig. 2), the drop in the μ_1 value results largely from the decrease in V_0 rather than in V_i . To a first approximation, observed narrowing of peaks can be related to the reduction in their retention (which is rather significant for the case under discussion). The difference in the dynamics of the μ_2 decrease for BD and DP is determined by a variation in the packed bed efficiency, i.e. the number of theoretical plates, N , or the height equivalent to the theoretical plate, H , as $\mu_2 = \mu_1^2/N$ or $\mu_2 = \mu_1^2 H/L$. The corresponding variations in N and H values for both substances are shown in Fig. 6 and Fig. 7, respectively. A different pattern of variation of these parameters for BD and PD is readily apparent. An essentially uniform decrease in N is observed for BD in the range of

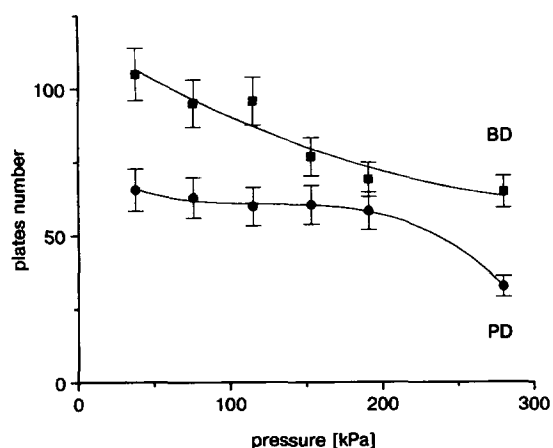


Fig. 6. Number of theoretical plates versus compression pressure: the lines correspond to second (BD) and third (PD) power polynomial regression fits.

compression pressure from 38 to 200 kPa, and this decrease becomes slower on further pressure elevation. In contrast, the slope of the N curve for PD increases at $P > 200$ kPa. It should be noted that the variation pattern of the H value also changes when compression pressure is elevated above 200 kPa.

In order to consider the observed differences in the plots of H versus P for BD and PD the well known Giddings expression [16] can be used. For SEC, the expression for H will be (thus sorption is supposed to be absent):

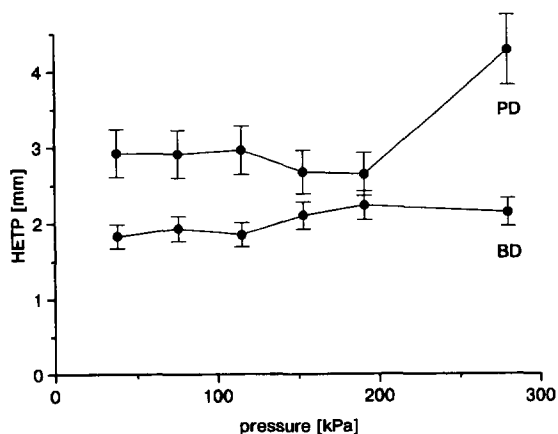


Fig. 7. HETP versus compression pressure.

$$H = H_L + H_{SM} + H_M = b \frac{D_M d_p}{u} + c_{SM} \frac{ud_p^2}{D_{SM}} + \frac{1}{1/ad_p + D_M/c_M ud_p^2} \quad (4)$$

where H_L , H_{SM} , and H_M are the plate height contributions due to longitudinal-diffusion, stationary-mobile-phase, and intra-particle mobile phase mass transfer processes, respectively; u is the linear flow-rate; d_p is the diameter of the packing particles, D_M and D_{SM} are solute-diffusion coefficients corresponding to extra-particle and stagnant mobile phase, respectively; a , b , c_{SM} are the coefficients of the respective dispersion terms, their magnitudes being generally a function of the nature and the geometry of packing and its pore structure.

Owing to a small D_M , H_L contribution to the overall plate height is negligible for BD. Besides, the linear flow-rate of the mobile phase increases with the reduction in packing porosity when compression is elevated, this results in a decrease in the H_L value. As dextran does not penetrate into the pores of packed beads, the corresponding H_{SM} value is equal to zero, and, in essence, its peak broadening depends only on its dispersion caused by inter-particle mobile phase mass transfer processes, described by the H_M term of Eq. 4.

H_M is a function of the linear flow-rate, u , and of the particle mean diameter, d_p . In the context of the random walk theory, the d_p value in the H_M term is used to represent the characteristic distances covered by various exchange processes between velocity extremes in the mobile phase. The magnitude of these distances is determined by the particle size as well as by averaged distances between their surfaces and/or centres. Bed compression results in a tighter packing that is equivalent to the reduction in the apparent d_p value in the H_M term or the corresponding variation in the values of a and c_M coefficients (provided the particle diameter is constant). It is very difficult to estimate this effect quantitatively because of the complexity of the description consistent with variations in the bed structure. It is worth mentioning that it has to result in the decrease in the H_M contribution to the overall plate height with u held constant. Alternatively, the flow-velocity increase corresponding to the operating conditions under discussion is known to cause the

H_M rise. The total effect of these opposite tendencies which are dependent on several parameters cannot be predicted easily. As shown in Fig. 7, these tendencies compensate for each other in the case of BD, and H remains practically constant upon compression. The observed H variations are comparable to the error value.

In the case of PD, H_L appears to contribute more markedly to the overall plate height than in the case of BD, the diffusion coefficient of PD being several orders of magnitude greater than the dextran D_M . For the same reason the pattern of H_M variation for PD upon bed compression can differ from that of BD. Besides, dispersion due to the stationary-mobile-phase mass transfer process (H_{SM} term) contributes essentially to H in the case of PD. The exact expression for H_{SM} according to the nonequilibrium theory [17] may be used for the description of the SEC stationary-phase dispersion in terms of geometrical parameters of the gel packing

$$H_{SM} = c_{SM} \frac{ud_p^2}{D_{SM}} = \frac{K_{SEC} V_i/V_0}{30(1 + K_{SEC} V_i/V_0)^2} \frac{ud_p^2}{D_{SM}} \quad (5)$$

where K_{SEC} is the SEC distribution coefficient. For PD, $K_{SEC}=1$, so if u and d_p are constant, the H_{SM} value is proportional to the $(V_i/V_0)/(1+V_i/V_0)^2$ ratio and must reduce with the increase (see Fig. 3) of the parameter V_i/V_0 . In order to take into account the influence of the flow-velocity increase on H_{SM} it is convenient to relate the former value to flow-rate and bed porosity. Since $V_0/Q=L/u$, where Q is the flow-rate, and $V_{col}=LS$, where V_{col} is the column volume, then u is equal to QV_{col}/SV_0 . Or, with $V_{col} \approx V_t$, linear flow velocity may be taken to be approximately proportional to V_i/V_0 or $(1+V_i/V_0)$ with an accuracy of Q/S constant. Thus if Q and d_p are kept constant, the H_{SM} value is proportional to the ratio $(V_i/V_0)/(1+V_i/V_0)$ and must increase with a V_i/V_0 rise. Fig. 8 depicts the curves illustrating variations in $(V_i/V_0)/(1+V_i/V_0)^2$ and $(V_i/V_0)/(1+V_i/V_0)$ ratios under changes of the V_i/V_0 parameter where the points mark their values corresponding to the experimental data on V_i/V_0 . The condition on d_p constancy is valid in the pressure range 0–200 kPa with V_i approximately equal to a constant. As compression increases further, V_i diminishes in a way that may be correlated with the deformation of particles and thus with

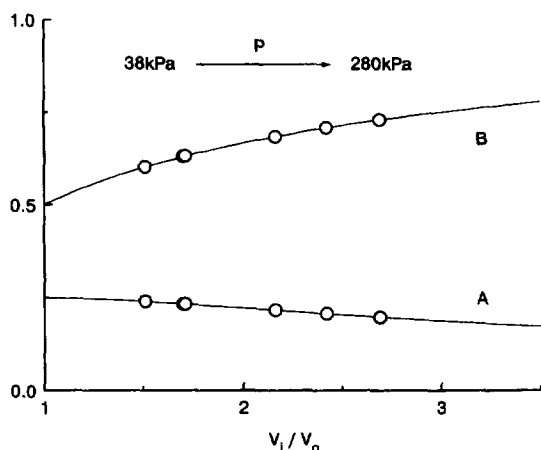


Fig. 8. Curves illustrating variation in (A) $(V_i/V_0)/(1+V_i/V_0)^2$ and (B) $(V_i/V_0)/(1+V_i/V_0)$. The points mark their values corresponding to the experimental data on V_i/V_0 .

variations in d_p and probably in D_{SM} . The combined effect of the variations of all these parameters on H_{SM} cannot be considered properly within the context of the approximation involved. As a result of the oppositely directed changes of separate components the overall H curve for PD appears to be of a rather complex shape (see Fig. 7).

The above consideration of the influence of compression on the plate height suggests that resolution can be further improved by holding the flow velocity, u , constant (at least for substances with a negligible contribution to HETP due to longitudinal diffusion). But the separation time will increase in this case, so the user has to choose between resolution and separation speed.

3.3. Peak asymmetry and resolution

As shown in Fig. 4, significant asymmetry is observed for both substances. Its value, expressed in terms of the σ/τ ratio, decreased substantially (1.84 times) for BD and remained constant within the experimental error for PD with increasing pressure on the packing (see Fig. 9). It is impossible to explain this effect in the context of the simplified random walk theory. Peak tailing may be attributed

to discontinuities in the flow pattern, which are reduced to a minimum due to bed consolidation upon compression. This conclusion is supported by the fact that the asymmetry decrease is observed only for substances excluded from the intra-particle volume. The expression for resolution corrected for peak asymmetry (R_s^*) has been used for the estimation of the separation quality of BD and PD:

$$R_s^* = \frac{V_M^1 - V_M^0}{\sigma_i + \tau_0}, \quad (6)$$

where V_M^0 and V_M^1 are the elution volumes of the BD and PD peak maxima, respectively.

The influence of contraction of the soft gel packing on peak separation is depicted in Fig. 10. The curve has a maximum in the 200-kPa region where the resolution exceeds its initial value 1.25 times. The observed variation in the given parameter can be easily explained. Dispersion of the chromatographic zones decreases (see Fig. 5) while the retention difference remains approximately constant as $V_M^1 - V_M^0 \approx \mu_1^1 - \mu_1^0 \approx V_i$.

If the distribution coefficient does not alter significantly under contraction of the gel bed (in the range where $V_i \approx \text{constant}$) then, with the constraint of peak narrowing, similar phenomena may be supposed to hold also for substances with $0 < K_{SEC} < 1$ since in this case the $\mu_1^{j+1} - \mu_1^j$ difference equal to $V_i (K_{SEC}^{j+1} - K_{SEC}^j)$ also remains approximately constant.

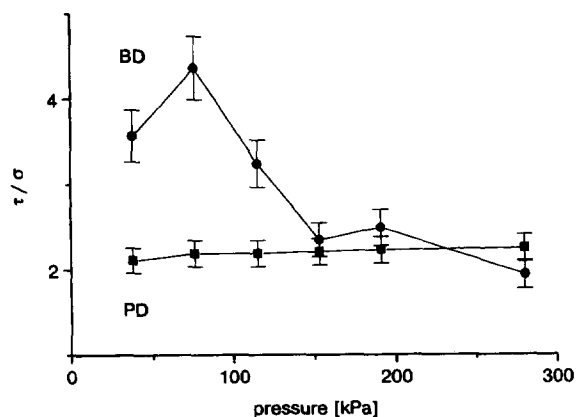


Fig. 9. Effect of axial compression on peak asymmetry.

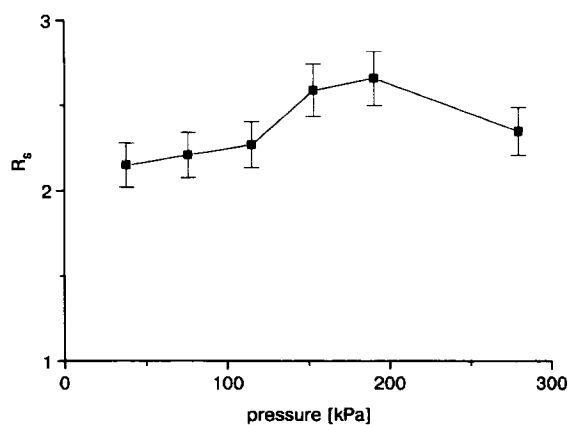


Fig. 10. Effect of axial compression on peak resolution.

4. Conclusion

The results obtained confirm that soft gel (Sephadex G-25) compression results in the improvement of chromatographic separation with a parallel reduction in its duration and eluent consumption. Theoretical interpretation of the soft gel behaviour provides general support for the positive influence of continuous axial compression on column performance. In order to gain insight into the details of the phenomena including compression optima and variations of chromatographic parameters of samples with $K_{SEC} < 1$, we are going to perform additional precise experiments incorporating process scaling and studies of other packing materials used for SEC.

References

- [1] E. Boschetti, *J. Chromatogr. A*, 658 (1994) 207.
- [2] G. Guiochon and A. Katti, *Chromatographia*, 24 (1987) 165.
- [3] M. Verzele, M. De Coninck, J. Vindevogel and C. Dewaele, *J. Chromatogr.*, 450 (1988) 47.
- [4] B. Porsch, *J. Chromatogr. A*, 658 (1994) 179.
- [5] G. Guiochon and H. Colin, in P. Kucera (Editor), *Microcolumn High-Performance Liquid Chromatography*, Elsevier, Amsterdam, 1984, p. 1.
- [6] H. Colin, P. Hilaireau and J. de Tournemire, *LC-GC*, 8 (1991) 302.
- [7] J.W. Little, R.L. Cotton, J.A. Pendergast and P.D. McDonald, *J. Chromatogr.*, 126 (1976) 439.
- [8] F. Godbille and P. Devaux, *J. Chromatogr. Sci.*, 12 (1974) 565.
- [9] G. Carta and W.B. Stringfield, *J. Chromatogr. A*, 658 (1994) 407.
- [10] D.-R. Wu and K. Lohse, *J. Chromatogr. A*, 658 (1994) 381.
- [11] M. Sarker and G. Guiochon, *J. Chromatogr. A*, 683 (1994) 293.
- [12] V.H. Edwards and J.M. Helft, *J. Chromatogr.*, 47 (1970) 490.
- [13] M.B. Baru and I.V. Kozlovsky-Vagenina, *J. Chromatogr. A*, 657 (1993) 199.
- [14] M.B. Baru, I.L. Rodionov, L.Ya. Shestakovsky and V.T. Larin, *Int. Pat. WO 88:89900366*, 9, July 29, 1988.
- [15] M.B. Baru and I.L. Rodionov, *Proceedings of the 2nd Japan Symposium on Peptide Chemistry*, ESCOM Science Publishers, Leiden, 1991, p. 119.
- [16] J.C. Giddings, *Dynamics of Chromatography, Part 1. Principles and Theory*, Marcel Dekker, New York, 1965, Ch. 2, p. 62.
- [17] J.C. Giddings, *Dynamics of Chromatography, Part 1. Principles and Theory*, Marcel Dekker, New York, 1965, Ch. 4, p. 147.